Magnetic Resonance Imaging 57 (2019) 303–312

Contents lists available at ScienceDirect

Magnetic Resonance Imaging

journal homepage: www.elsevier.com/locate/mri

Original contribution

# Rigid motion correction for magnetic resonance fingerprinting with sliding-window reconstruction and image registration☆,☆☆

Zhongbiao Xu[a,b,1], Huihui Ye[c,e,1], Mengye Lyu[d], Hongjian He[e], Jianhui Zhong[e], Yingjie Mei[a,b,f], Zhifeng Chen[a,b,1], Ed X. Wu[d], Wufan Chen[a,b], Qianjin Feng[a,b], Yanqiu Feng[a,b,*]

[a] Key Laboratory of Mental Health of the Ministry of Education, School of Biomedical Engineering, Southern Medical University, Guangzhou, China
[b] School of Biomedical Engineering, Guangdong Provincial Key Laboratory of Medical Image Processing, Southern Medical University, Guangzhou, China
[c] State of Key Laboratory of Modern Optical Instrumentation, College of Optical Science and Engineering, Zhejiang University, Hangzhou, China
[d] Laboratory of Biomedical Imaging and Signal Processing, University of Hong Kong, Hong Kong, China
[e] Center for Brain Imaging Science and Technology, Key Laboratory for Biomedical Engineering of Ministry of Education, Zhejiang University, Hangzhou, China
[f] Philips Healthcare, Guangzhou, China

ARTICLE INFO

*Keywords:*
Magnetic resonance fingerprinting
Sliding-window reconstruction
Motion correction
Image registration

ABSTRACT

Magnetic resonance fingerprinting (MRF) can be used to simultaneously obtain multiple parameter maps from a single pulse sequence. However, patient motion during MRF acquisition may result in blurring and artifacts in estimated parameter maps. In this work, a novel motion correction method was proposed to correct for rigid motion in MRF. The proposed method involved sliding-window reconstruction to obtain intermediate images followed by image registration to estimate rigid motion information between these images. Finally, the motion-corrupted k-space data were corrected with the estimated motion parameters and then reconstructed to obtain the parameter maps via the conventional MRF processing pipeline. The proposed method was evaluated using both simulations and in vivo MRF experiments with intently different types of motion. For motion-corrupted data, the proposed method yielded brain $T_1$, $T_2$ and proton density maps with obviously reduced blurring and artifacts and lower normalized root-mean-square error, compared to MRF without motion correction. In conclusion, motion-corrected MRF using the proposed method has the potential to produce accurate parameter maps in the presence of in-plane rigid motion.

## 1. Introduction

Magnetic resonance fingerprinting (MRF) [1] provides a quantitative imaging method for a rapid and simultaneous measurement of multiple tissue-related quantitative parameters, such as $T_1$, $T_2$ and proton density (PD). The reconstruction of MRF mainly consists of three steps: 1) acquiring signal temporal evolutions with a series of varying repetition times (TRs) and flip angles (FAs); 2) constructing a dictionary of signal evolutions by Bloch equation or extended phase graphs (EPG) [2,3] simulation with different combinations of tissue parameters, such as $T_1$ and $T_2$; and 3) estimating parameter maps by matching acquired signal evolutions to items in the constructed dictionary.

A number of methods have been developed to improve the accuracy and efficiency of MRF. The accuracy of MRF is increased by improving the quality of images reconstructed from highly undersampled k-space data through iteration-based multiscale reconstruction [4], sliding-window reconstruction [5], sparse reconstruction [6] and low-rank constrained reconstruction [7–9]. Two-dimensional MRF acquisition is substantially accelerated by using simultaneous multi-slice imaging technique that simultaneously excites multiple slices with multiband pulses [10]. Recently, singular value decomposition (SVD) and group matching methods have been developed to compress the dictionary for speeding up the template matching operation in MRF [11,12] by exploiting the strong correlation along the time or parameter dimension of simulated dictionary.

Motion during data acquisition hinders accurate and robust MRF. MRF shows insensitivity to motion during the late stage of the acquisition [1]. However, motion during the early and middle stages of the

☆ This work has not been published previously, will not be submitted elsewhere while under review at the Magnetic Resonance Imaging, and has been approved by all authors.

☆☆ Conflicts of interest: none.

* Corresponding author at: School of Biomedical Engineering, Southern Medical University, Guangzhou, China.
*E-mail address:* foree@163.com (Y. Feng).

[1] These authors contributed equally to this work.

https://doi.org/10.1016/j.mri.2018.11.001
Received 15 August 2018; Received in revised form 8 October 2018; Accepted 11 November 2018

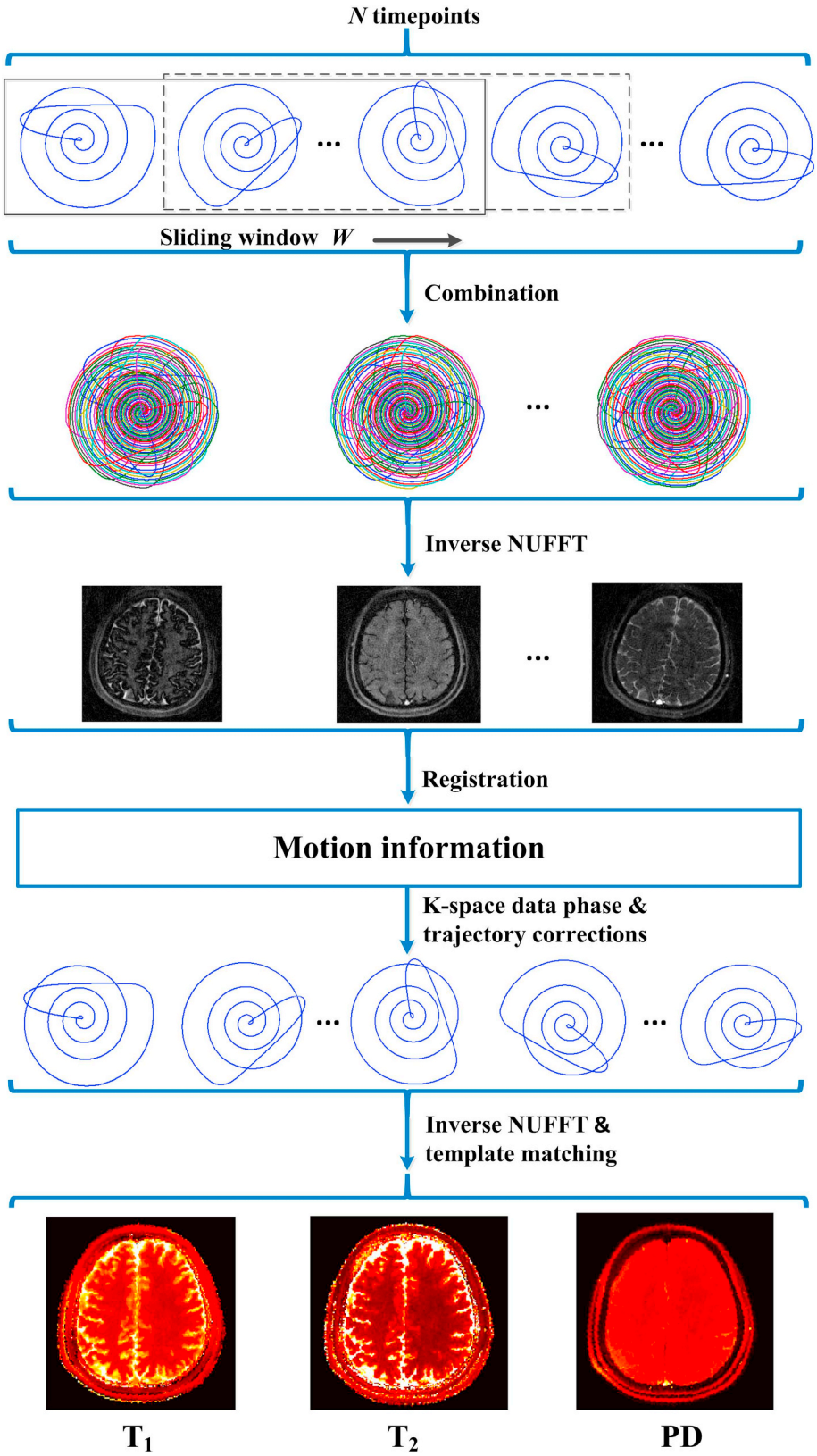


**Fig. 1.** Flowchart of the proposed motion correction method for MRF. Inverse nonuniform fast Fourier transform (NUFFT) was used for image reconstruction.

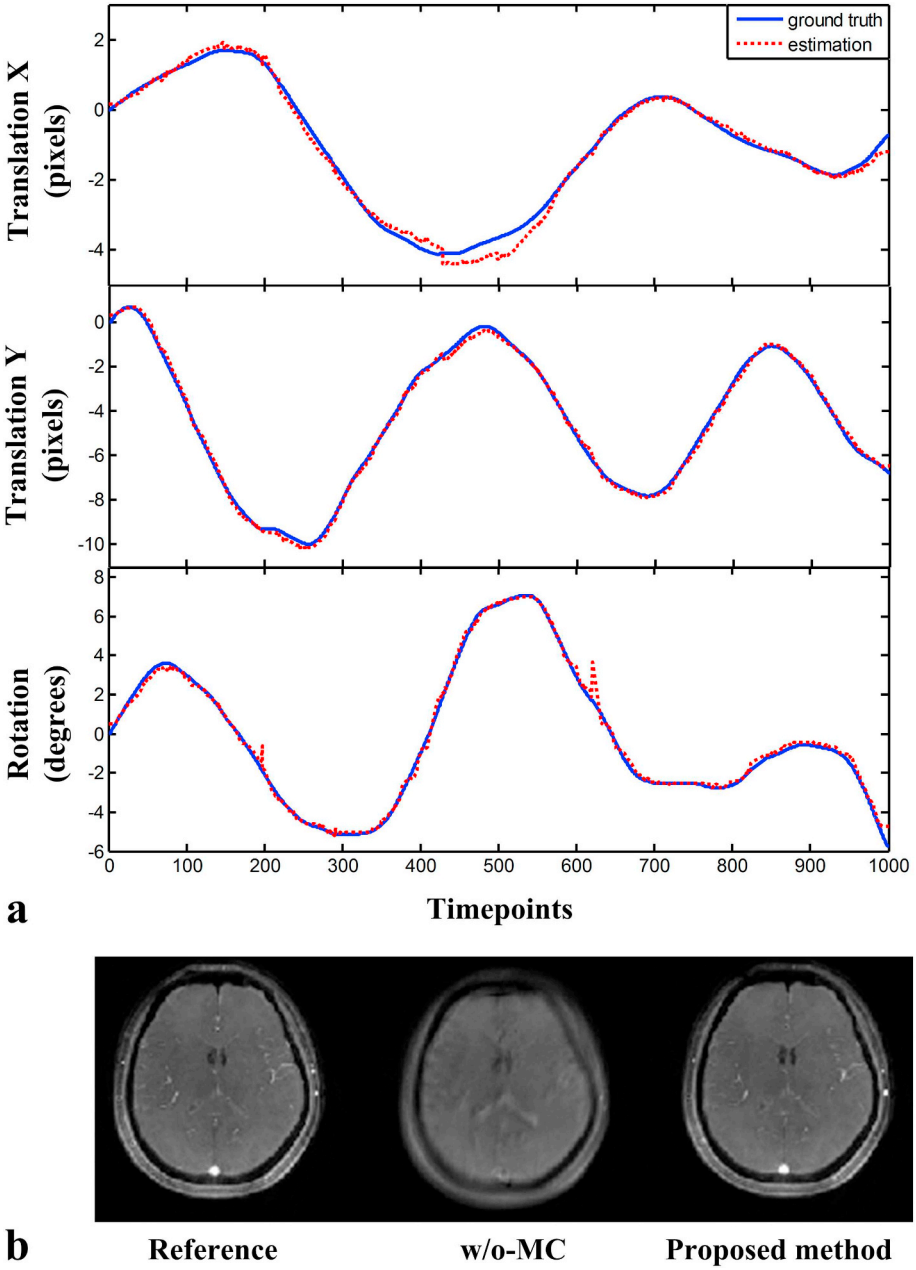


**Fig. 2.** Accuracy of motion estimation and reconstruction results of the simulated experiment. (a) Comparison between ground truth (solid line) and estimated motion (dotted line). (b) Complex averages of 1000 frames reconstructed with MRF without motion correction (w/o-MC) and the proposed method.

acquisition can cause severe blurring and artifacts in estimated parameter maps [13–16]. Several methods have been recently developed to correct for bulk patient motion during the MRF acquisition. Mehta et al. [13] proposed to correct for motion in MRF by iteratively performing dictionary matching, motion estimation and correction, and image reconstruction. In this method, the dual-density spiral acquisition is adopted to acquire sufficient data in the central k-space region for accurate motion estimation. It is challenging to robustly extract accurate motion information from highly-undersampled data of each interleaf in MRF. Recently, Cruz et al. [14] and Xu et al. [15] have developed an MRF motion correction approach which obtains intermediate images with less aliasing artifacts by using the sliding-window reconstruction.

This study is an extension of our preliminary work published in a conference proceeding [15]. The motion information was estimated from sliding-window intermediate images by using image registration. With registration-estimated parameters, the effect of motion was corrected in the k-space domain. Finally, the motion-corrected k-space data were reconstructed to obtain motion-free parameter maps by using the original MRF processing pipeline. The performance of the proposed method was validated on both simulation and in vivo brain data.

## 2. Methods

### 2.1. Proposed method

To address the effect of motion-induced spatial mismatch on parameter estimation in MRF, the proposed method firstly used a sliding-window reconstruction to obtain individual images with improved quality for accurate motion estimation. These intermediate images were then co-registered by using image registration to estimate motion parameters. Finally, the k-space data were corrected with the estimated motion and then reconstructed to obtain motion-free parameter maps

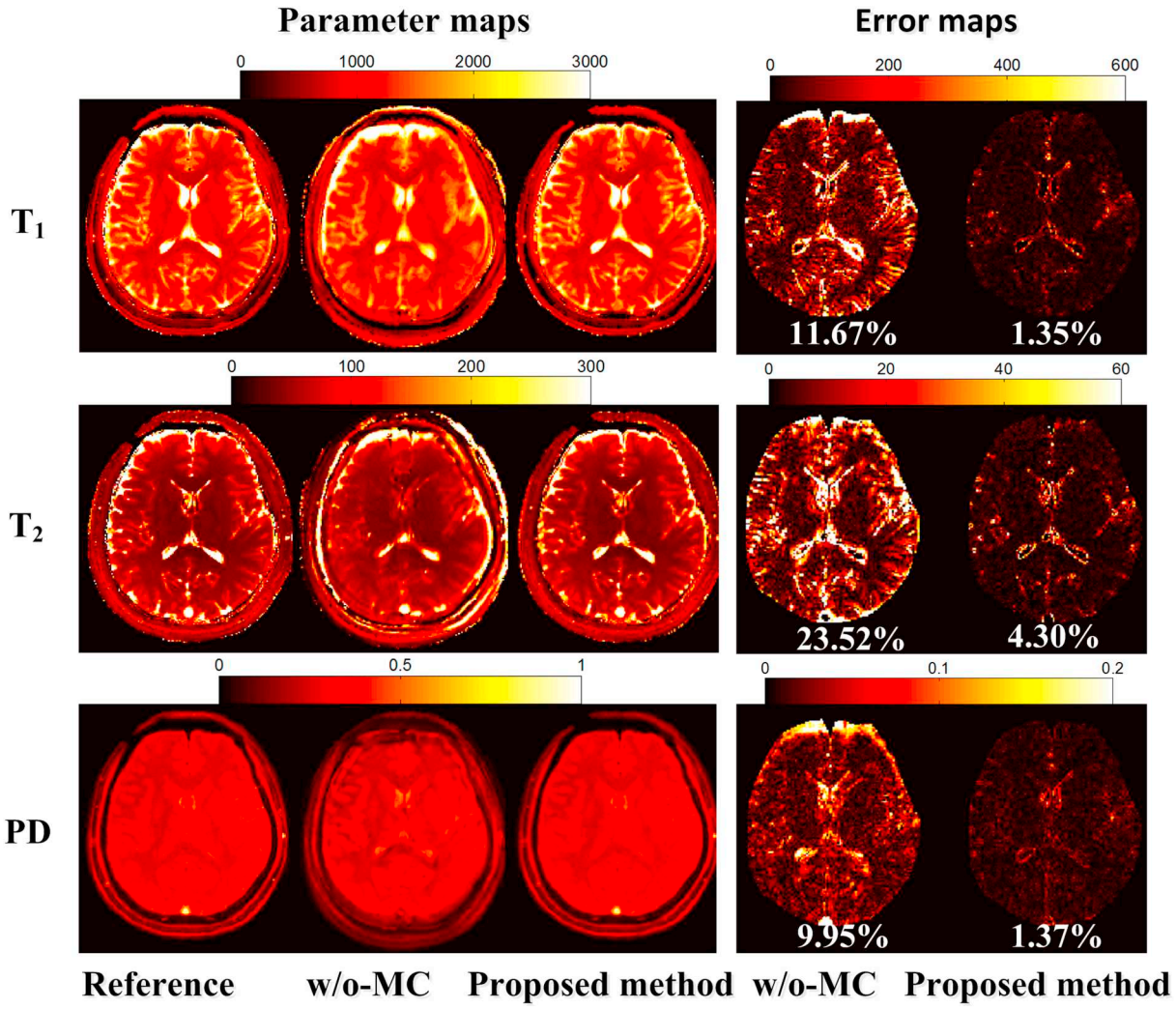


**Fig. 3.** $T_1$, $T_2$ and PD maps, and the corresponding error maps estimated with MRF without motion correction (w/o-MC) and the proposed method from the simulated experiment with continuous in-plane motion. The nRMSEs were calculated and listed at the bottom of the corresponding error maps.

via the established MRF pipeline. Fig. 1 depicts the framework of the proposed motion correction method for MRF. A detailed explanation is as follows.

*2.1.1. Sliding-window reconstruction*

In MRF, timeframes reconstructed from individual spiral readouts usually contain strong aliasing artifacts because of high under-sampling factors, which compromise the accuracy of motion estimation. To address this problem, we reconstructed each timeframe by combining a fixed number of consecutive multiple interleaves in a sliding-window fashion [5]. The sliding-window reconstruction can obtain high-quality images with reduced artifacts for the following motion estimation. In this study, the sliding window width $W$ was experimentally set at 16.

*2.1.2. Motion estimation and correction*

The proposed method estimated motion information by performing 2D rigid registration between the intermediate images from the previous step and the mutual information was chosen as similarity metric, which is insensitive to contrast variations between images [17]. Because of residual aliasing artifacts and motion artifacts in the intermediate images, registration with a single reference may lead to large motion estimation errors. Therefore, group-based registration was used to estimate motion parameters. The intermediate images were divided into several groups by clustering temporally adjacent images, and intra-group registration was performed. The registered images in each group were then averaged to form a complex average image, which has significantly reduced artifacts compared with individual intermediate images. Finally, inter-group registration was performed on these complex average images. Consequently, the motion information of each individual image can be obtained by summing the corresponding motion parameters from intra-group and inter-group registration. In this study, every 70 consecutive images were regarded as one group. The image having the strongest correlation with other images was regarded as reference during intra-group and inter-group registration.

The registration-estimated parameters were applied to the raw k-space data for motion correction. Specifically, the translational motion and rotational motion were corrected by modifying the phase of k-space data and the corresponding k-space trajectory [18], respectively.

*2.1.3. Parameter estimation*

The $T_1$, $T_2$ and PD maps were obtained by performing the original MRF pipeline [1] on the corrected k-space data. To accelerate the template matching procedure in MRF, SVD was used to compress dictionary and signals along the time dimension [11] and the first 40 singular vectors were reserved in this step.

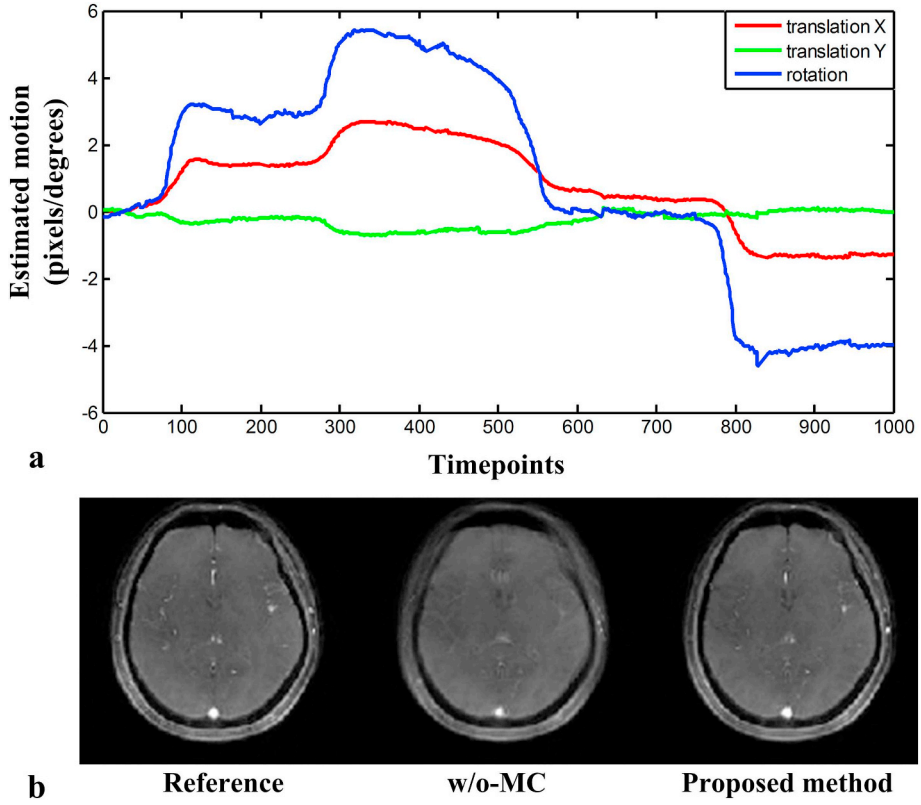


**Fig. 4.** Estimated motion (a) and reconstructed complex average images of 1000 frames (b) from the in vivo experiment with intermittent in-plane motion with MRF without motion correction (w/o-MC) and the proposed method.

### 2.2. Experiments

All experimental datasets were acquired on a 3.0 Tesla MAGNETOM Prisma scanner (Siemens Healthcare, Erlangen, Germany) with a 16-channel head coil. The inversion-recovery fast imaging with steady state precession sequence (FISP) [19], where the unbalanced gradient within each TR was applied to the slice-selection direction, was used for MRF data acquisition. TRs varied from 11.27 ms to 13.93 ms and FAs ranged from 5° to 70°. Nine FAs with zero degree were inserted every 200 timepoints for magnetization recovery. Variable density spiral trajectory was used and the spiral trajectory rotated a golden angle [20,21] at each TR. The acceleration factor was 24 for the center of k-space and 48 for the edge of k-space. The other scan parameters were as follows: field of view = 300 × 300 $mm^2$, in-plane resolution = 1.17 × 1.17 $mm^2$, fixed echo time = 3.0 ms, slice thickness = 5 mm, number of slices = 5 and number of timepoints = 1000. All human studies were performed under Institutional Review Board approval and informed consent was obtained from the volunteer before MRI scan.

To evaluate the effectiveness of the proposed method, simulated and in vivo experiments were conducted. For simulation, synthesized continuous motion was added to a set of acquired static data by modifying the raw k-space data [18] to obtain the motion-corrupted datasets. The noise in the simulated data is from that in the in vivo data, and no additional noise was added. Moderate (Fig. 2a) and drastic (Supporting Fig. S1a) motion experiments were simulated, respectively. In the moderate motion experiment, the motion ranged from −4 to 1.7 pixels for translation X, −10 to 0.67 pixels for translation Y, and −5.8° to 7° for rotation; in the drastic motion experiment, the motion ranged from −5.15 to 4.8 pixels for translation X, −2.4 to 2.57 pixels for translation Y, and −8.58° to 8° for rotation. For in vivo experiments, the volunteer was instructed to perform four scans: 1) no motion, 2) intermittent in-plane motion (yaw), 3) continuous in-plane motion (yaw), and 4) continuous combined in-plane and through-plane motion (yaw and nodding). Results from motion-free data were regarded as references.

### 2.3. Image reconstruction

To accelerate the reconstruction, 16-channel data were compressed to 6-channel data by using coil compression [22,23]. Then, the inverse nonuniform fast Fourier transform (NUFFT) [24] was used to reconstruct the compressed datasets. Coil sensitivity profiles were estimated from the first 200 timepoints data by ESPIRiT [25] and then used for the combination of multi-channel images. The step size of the sliding-window was set at 1, and a total of 985 high-quality images were reconstructed with the sliding-window reconstruction for each dataset. The registration of images for motion estimation was performed by using MATLAB's image registration toolbox. The dictionary based on the sequence was generated by EPG [2,3]. $T_1$ values ranged from 100 ms to 3000 ms with a step of 20 ms, and $T_2$ values ranged from 10 ms to 300 ms with a step of 5 ms. Signals with $T_1$ less than $T_2$ were excluded from the dictionary. The inner product as described in the original MRF was used for template matching between acquired signal evolutions and dictionary items. All postprocessing steps were implemented in MATLAB (Mathworks, Natick, Massachusetts, USA) installed on a Windows machine (3.2 GHz CPU, 8 GB RAM).

### 2.4. Quantitative evaluation

The normalized root-mean-square error (nRMSE) in a manually defined region-of-interest (ROI) was calculated for the quantitative performance evaluation:

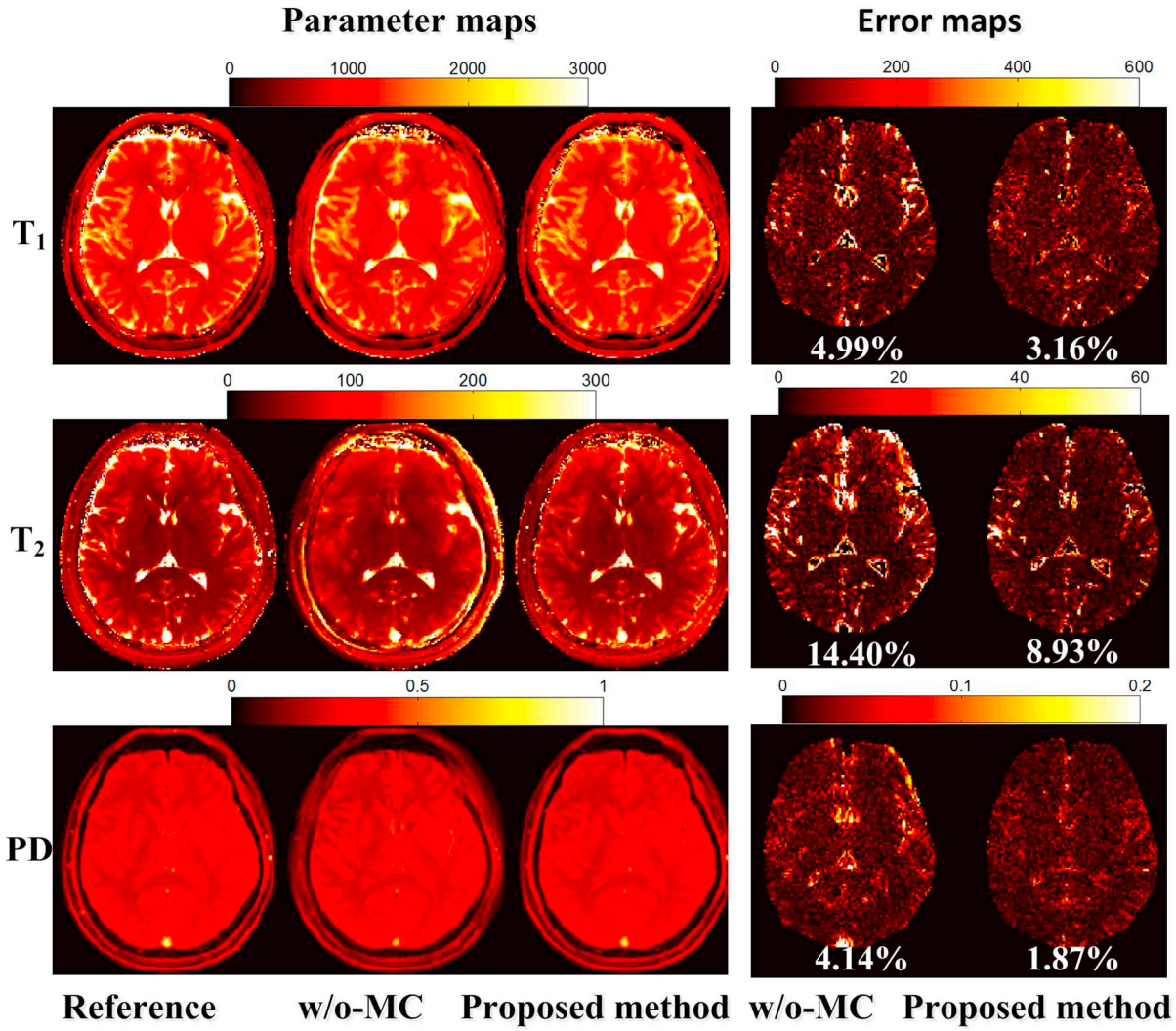


**Fig. 5.** $T_1$, $T_2$ and PD maps, and the corresponding error maps estimated with MRF without motion correction (w/o-MC) and the proposed method from the in vivo experiment with intermittent in-plane motion. The nRMSEs were calculated and listed at the bottom of the corresponding error maps.

$$nRMSE = \sqrt{\frac{\sum_{l\in \mathrm{ROI}} (\widehat{\mathbf{P}}(l) - \mathbf{P}_{\mathrm{ref}}(l))^2}{\sum_{l\in \mathrm{ROI}} (\mathbf{P}_{\mathrm{ref}}(l))^2}}$$

where $l$ is the pixel index in the ROI, $\widehat{\mathbf{P}}$ the parameter map estimated from the motion-corrupted data, and $\mathbf{P}_{\mathrm{ref}}$ the reference parameter map estimated from the no motion data. In this study, a manually-drawn whole brain ROI without background and skull was used for the calculation and comparison of nRMSE.

## 3. Results

### 3.1. Simulation

Figs. 2–3 show the application of the proposed method to simulated MRF data with moderate motion. The motion (translations and rotation) parameters estimated by the proposed method are plotted in Fig. 2a. The proposed method obtains motion parameters close to the ground truth. The large rotation estimation error for several timepoints is because these timepoints correspond to the acquisition with zero degree FA. The estimation errors (mean and standard deviation) are $0.14 \pm 0.14$ pixels for translation X, $0.12 \pm 0.08$ pixels for translation Y, and $0.13 \pm 0.14^{\circ}$ for rotation. Fig. 2b presents the complex averages of 1000 frames reconstructed without and with motion correction. The average image without motion correction (w/o-MC) contains severe blurring. In contrast, the average image with motion correction using the proposed method exhibits no obvious blurring and is closer to the reference image. With regard to MRF parameter maps, as shown in Fig. 3, the proposed method successfully removes the motion-caused blurring and artifacts in the $T_1$, $T_2$ and PD maps and obtains minimal residual errors. Quantitatively, compared with MRF without motion correction, the proposed method achieves lower nRMSEs, which were calculated in the whole image and listed at the bottom of the corresponding error maps. The motion correction by the proposed method reduces nRMSE from 11.67% to 1.35% for $T_1$ map, 23.52% to 4.30% for $T_2$ map, and 9.95% to 1.37% for PD map. The results of simulated experiments with drastic motion are shown in Supporting Figs. S1–S2.

The reconstruction time for one typical slice is approximately 10 min. The time costs of each main procedure are listed as follows. The reconstruction of image series of 1000 timepoints took 2 min 30 s. The image registration took 7 min 13 s. The cost of coil sensitivities estimation and template matching was 25 s.

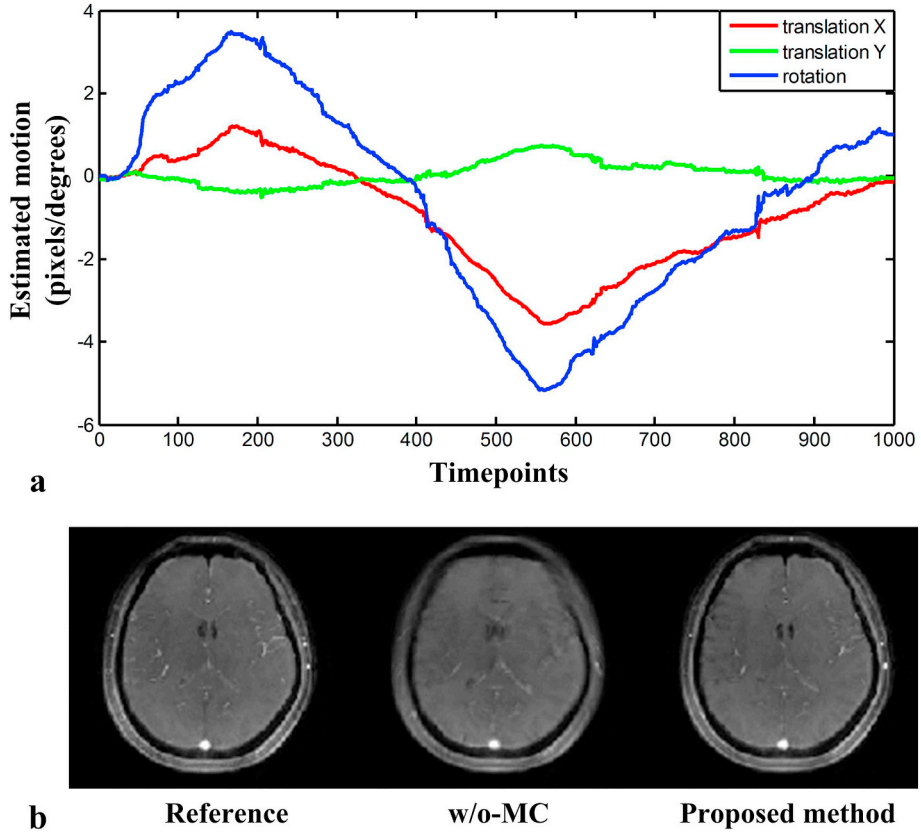


**Fig. 6.** Estimated motion (a) and reconstructed complex average images of 1000 frames (b) from the in vivo experiment with continuous in-plane motion with MRF without motion correction (w/o-MC) and the proposed method.

### *3.2. In vivo brain MRF*

The results of one representative slice of the in vivo experiments with intermittent in-plane motion are presented in Figs. 4–5. Fig. 4a shows the estimated motion information. Four movements are detected and the estimated motion ranges from −1.69 to 2.72 pixels for translation X (left–right direction), −0.67 to 0.21 pixels for translation Y (posterior–anterior direction), and −4.56° to 5.46° for rotation. As shown in Fig. 4b, the complex average image of the original 1000 frames is severely corrupted with motion-related blurring and artifacts, while the average of motion-corrected images by the proposed method presents no blurring and artifacts. Fig. 5 shows the corresponding $T_1$, $T_2$ and PD maps, and the error maps. Noticeable blurring and artifacts can be observed in the $T_1$, $T_2$ and PD maps from MRF without motion correction. In contrast, MRF with motion correction using the proposed method obtains accurate parameter maps without obvious blurring and artifacts. The quantitative nRMSEs were calculated and listed at the bottom of the corresponding error maps. The proposed method produces a lower nRMSE in parameter mapping (3.16% vs. 4.99% for $T_1$ map, 8.93% vs. 14.40% for $T_2$ map, and 1.87% vs. 4.14% for PD map) than MRF without motion correction.

Figs. 6–7 show the results of one typical slice of the in vivo experiments with continuous in-plane motion. The estimated in-plane motion, as shown in Fig. 6a, ranges from −3.56 to 1.20 pixels for translation X (left–right direction), −0.40 to 0.74 pixels for translation Y (posterior–anterior direction), and −5.16° to 3.48° for rotation. The proposed method successfully captured the continuous yaw motion performed by the volunteer. With regard to the average images (Fig. 6b) and estimated parameter maps (Fig. 7), the blurring and artifacts are observed again in the parameter maps generated by MRF without motion correction. The proposed method effectively removes motion-related blurring and artifact and thus obtains less residual errors. Quantitatively, the proposed method decreases nRMSE from 5.55% to 2.37% for $T_1$ map, 20.53% to 13.72% for $T_2$ map, and 3.54% to 1.99% for PD map.

The application of the proposed method to continuous combined in-plane and through-plane motion is shown in Fig. 8. The $T_2$ and PD maps generated by the proposed method are significantly different from those from stationary data. Compared with MRF without motion correction, the proposed method corrected for the existing in-plane motion and thus substantially reduced blurring and artifacts and generated parameter maps with lower nRMSEs (6.77% vs. 9.13% for $T_1$ map, 43.53% vs. 44.64% for $T_2$ map, and 9.32% vs. 10.45% for PD map). The estimated in-plane motion is shown in Supporting Fig. S3.

## 4. Discussion

In this study, we presented a novel motion correction method for MRF. The proposed method estimates motion information by registering intermediate images reconstructed in a sliding-window fashion, and then corrects the k-space data with the estimated motion to obtain motion-free parameter maps using the conventional MRF framework. The simulation and in vivo results demonstrate that the proposed method can retrospectively suppress motion artifacts and improve the accuracy of parameter maps in comparison to MRF without motion correction in the presence of in-plane motion. For the case of through-plane motion, though residual artifacts still existed, improved parametric maps were obtained by the proposed method.

The accuracy of motion estimation is vital for the performance of the proposed method and depends on the quality of images to be registered, which is closely related to the width of sliding window. The images reconstructed from individual interleaves in MRF usually contain severe aliasing artifacts, and the registration of these images is very challenging and usually obtains inaccurate motion estimation. The

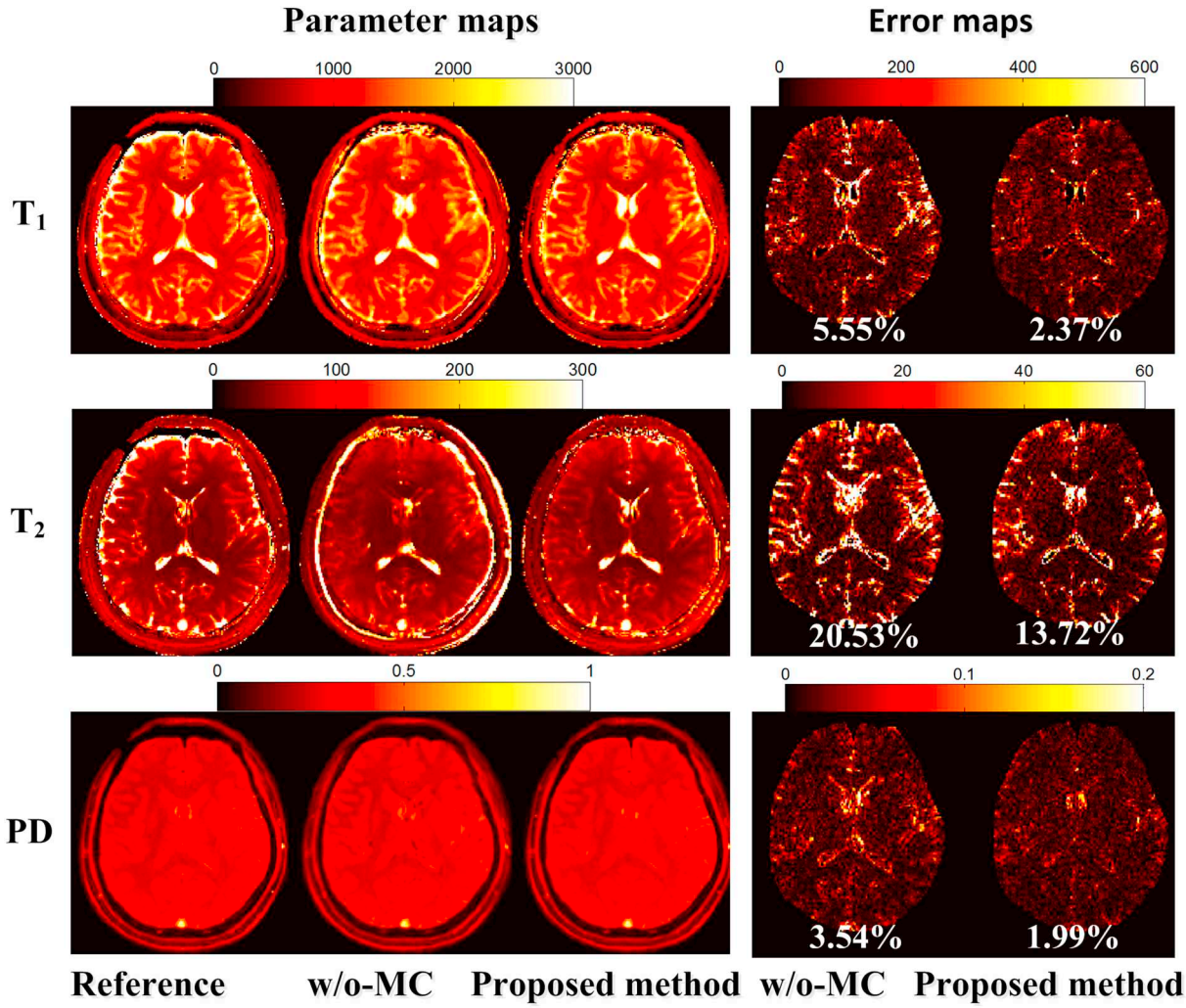


**Fig. 7.** $T_1$, $T_2$ and PD maps, and the corresponding error maps estimated with MRF without motion correction (w/o-MC) and the proposed method from the in vivo experiment with continuous in-plane motion. The nRMSEs were calculated and listed at the bottom of the corresponding error maps.

aliasing artifacts can be reduced by using the sliding-window reconstruction, but with an increased risk of motion artifacts because of reduced temporal resolution. Thus, the sliding-window width needs to be chosen carefully to compromise the aliasing artifacts and motion artifacts in the intermediate images. Supporting Fig. S4 shows the results of the simulation experiment with moderate in-plane motion reconstructed by using the proposed method with varying sliding-window widths. At the sliding-window width of 4, obvious artifacts were observed in the $T_2$ and PD maps. MRF accuracy increased as the sliding-window width was increased from 4 to 16. Further increasing the sliding-window width resulted in a slight reduction of MRF accuracy. Though the sliding-window width $W$ of 16 is optimal in the current simulation experiments, the optimal value may vary with motion patterns and frequencies. For infrequent motion, the sliding-window reconstruction with a large widow width $W$ may help to increase the signal-to-noise ratio (SNR) of intermediate images and improve the accuracy of motion estimation. With regard to frequent or continuous motion, a small $W$ is preferred because it can help to reduce the effect of motion on intermediate images. The optimization of the window width for varying motion patterns and frequencies needs to be investigated in future work.

With variable FAs in MRF, each spiral acquisition will have different SNRs and thus the images from sliding-window reconstruction will also have variable SNRs. Low SNR can potentially reduce the accuracy of motion estimation as shown in Fig. 2a and Supporting Fig. S1a where large motion estimation errors were observed at the timepoints with low SNR due to zero degree FA. Though the simulation experiments with noise from in vivo data demonstrated that the motion estimation is accurate except for the timepoints with zero degree FA, the investigation on the experiments with lower SNR would be of interest in future work. Currently, the proposed method reconstructed intermediate image series by directly applying inverse NUFFT to acquired non-Cartesian data. The quality of intermediate images can be further improved by introducing sparsity-constrained reconstruction techniques [26,27] to improve motion estimation accuracy.

The accuracy of motion estimation also depends on the adopted image registration method. The intermediate images reconstructed by using the sliding-window method still contain residual artifacts, and their contrast may substantially vary with signal evolution, compromising the accuracy of image registration. The proposed method divided these intermediate images into several groups. After intra-group registration, the registered images were averaged to obtain a representative image with significantly reduced artifacts for each group. The average images were used in the following inter-group registration to improve the accuracy of motion estimation. In this study, we classified 70 consecutive images into one group. The effect of group method on the accuracy of registration is of interest in the future work. The groupwise registration method [28] which avoids the bias towards to a single reference by simultaneously aligning all images is a promising registration method for further improving the accuracy of motion estimation.

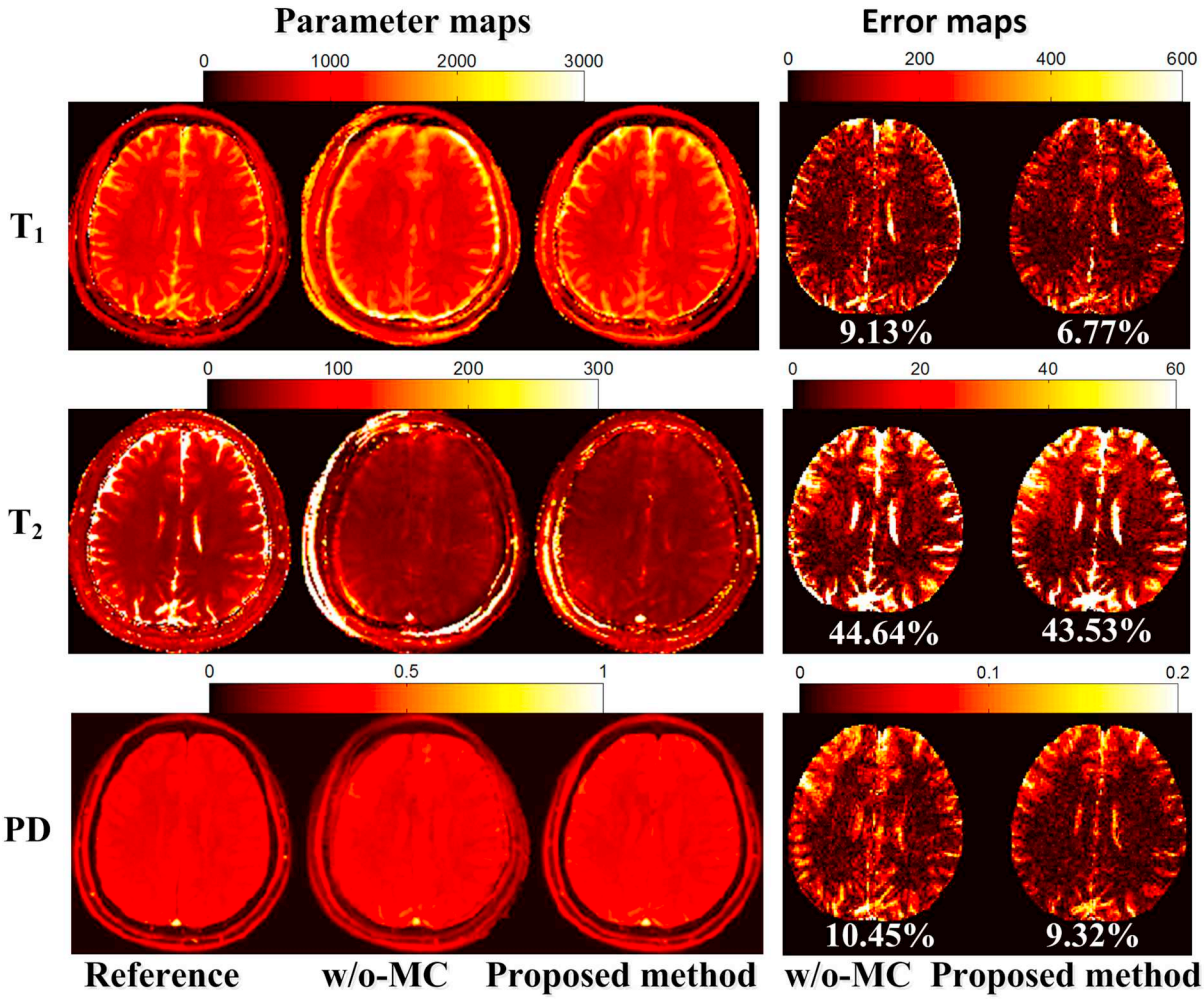


**Fig. 8.** $T_1$, $T_2$ and PD maps, and the corresponding error maps estimated with MRF without motion correction (w/o-MC) and the proposed method from the in vivo experiment with continuous combined in-plane and through-plane motion. The nRMSEs were calculated and listed at the bottom of the corresponding error maps.

In the employed spoiled FISP sequence, motion changes the phase of each individual spin and stimulated echo. The complex sum of those echoes consequently changes overall signal evolution, biasing the relaxation times. This effect needs to be incorporated in the dictionary in the future work. Alternatively, the balanced steady state free-precession sequence can also be used to mitigate this effect dramatically [1]. Due to the existing unbalanced gradient, it is almost inevitable that through slice motion will alter the spin evolution and deteriorate the $T_2$ values (possibly in an irrecoverable way – effectively spoiling the signal) [16]. So 2D rigid-body motion correction may not totally eliminate the effects of motion, especially when they change during acquisition, motion occurring at different intervals during the flip angle train have different effects on the values measured using MRF.

In this study, the proposed motion correction method was implemented on MRF with 2D acquisition, and thus its current implementation only partly corrects for the through-plane motion (Fig. 8). The through-plane motion would lead to a further reduction in the accuracy of estimated in-plane motion parameters. Another effect of through-plane motion on the 2D MRF is that tissues inside a formerly excited slice may move outside the imaging slice and thus will not be excited by the following radiofrequency pulses. In addition, the unexcited tissues outside a formerly excited slice may enter the imaging slice and be excited by following radiofrequency pulses. That is to say, the through-plane motion introduces additional variations to signal evolutions that cannot be described by the simulated MRF dictionary. This effect will result in additional errors in MRF, especially for $T_2$ map [16]. Actually, the proposed motion correction method can be combined with 3D MRF acquisition [29,30] to address through-plane motion. Another potential through-plane motion correction method for MRF is the prospective approaches using information from external motion-tracking devices [31–33], which can be applied to both 2D and 3D MRF.

The proposed method took approximately 10 min to reconstruct one typical slice and the reconstruction time is too long for clinical use. The current implementation is based on MATLAB script. In the future, the corresponding C/C++ programming language can be used to accelerate the reconstruction. The computation time can be further reduced using parallel computation on Graphical Processing Units.

## 5. Conclusion

We proposed a novel motion correction method based on sliding-window reconstruction and image registration for MRF. Both simulated and in vivo experiments demonstrated that the proposed method can reduce motion-related artifacts and blurring in parameter maps and provide similar $T_1$, $T_2$ and PD maps to those from stationary data. The proposed method improves the robustness of MRF in the presence of motion and is expected to benefit the quantitative multiparameter imaging in the future.

## Acknowledgements

This work was supported by National Natural Science Foundation of China [61471188, 61671228, 61728107, 61701436, 61801205, and 91632109], National Key Technology R&D Program of China [2015BAI01B03], Technology R&D Program of Guangdong [2017B090912006] and China Postdoctoral Science Foundation [2018M633073].

## Conflicts of interest

None.

## Appendix A. Supplementary data

Supplementary data to this article can be found online at https://doi.org/10.1016/j.mri.2018.11.001.

## References

[1] Ma D, Gulani V, Seiberlich N, Liu K, Sunshine JL, Duerk JL, et al. Magnetic resonance fingerprinting. Nature 2013;495(7440):187–192.
[2] Weigel M, Schwenk S, Kiselev VG, Scheffler K, Hennig J. Extended phase graphs with anisotropic diffusion. J Magn Reson 2010;205(2):276–85.
[3] Weigel M. Extended phase graphs: dephasing, RF pulses, and echoes - pure and simple. J Magn Reson Imaging 2015;41(2):266–95.
[4] Pierre EY, Ma D, Chen Y, Badve C, Griswold MA. Multiscale reconstruction for MR fingerprinting. Magn Reson Med 2016;75(6):2481–92.
[5] Cao X, Liao C, Wang Z, Chen Y, Ye H, He H, et al. Robust sliding-window reconstruction for Accelerating the acquisition of MR fingerprinting. Magn Reson Med 2017;78(4):1579–88.
[6] Davies M, Puy G, Vandergheynst P, Wiaux YA. Compressed Sensing Framework for Magnetic Resonance Fingerprinting. Siam J Imaging Sci 2014;7(4):2623–56.
[7] Zhao B, Setsompop K, Adalsteinsson E, Gagoski B, Ye H, Ma D, et al. Improved magnetic resonance fingerprinting reconstruction with low-rank and subspace modeling. Magn Reson Med 2018;79(2):933–42.
[8] Mazor G, Weizman L, Tal A, Eldar YC. Low rank magnetic resonance fingerprinting. Proceedings of the 38th Annual International Con-ference of the IEEE Engineering in Medicine and Biology Society, Orlando, USA. 2016. p. 439–442.
[9] Assländer J, Cloos MA, Knoll F, Sodickson DK, Hennig J, Lattanzi R. Low rank alternating direction method of multipliers reconstruction for MR fingerprinting. Magn Reson Med 2018;79(1):83–96.
[10] Ye H, Cauley SF, Gagoski B, Bilgic B, Ma D, Jiang Y, et al. Simultaneous multislice magnetic resonance fingerprinting (SMS-MRF) with direct-spiral slice-GRAPPA (ds-SG) reconstruction. Magn Reson Med 2017;77(5):1966–74.
[11] McGivney DF, Pierre E, Ma D, Jiang Y, Saybasili H, Gulani V, et al. SVD compression for magnetic resonance fingerprinting in the time domain. IEEE Trans Med Imaging 2014;33(12):2311–22.
[12] Cauley SF, Setsompop K, Ma D, Jiang Y, Ye H, Adalsteinsson E, et al. Fast group matching for MR fingerprinting reconstruction. Magn Reson Med 2015;74(2):523–528.
[13] Mehta BB, Ma D, Coppo S, Griswold MA. Image reconstruction algorithm for motion insensitive MR Fingerprinting (MRF): MORF. Magn Reson Med 2018. https://doi.org/10.1002/mrm.27227.
[14] Cruz G, Botnar RM, Prieto C. Motion corrected Magnetic Resonance Fingerprinting using Soft-weighted key-Hole (MRF-McSOHO). Proceedings of the 25th Annual Meeting of ISMRM, Honolulu, Hawii, USA. 2017. p. 935.
[15] Xu Z, Lyu M, Hui E, Mei Y, Chen Z, Chen W, et al. Motion Correction for Magnetic Resonance Fingerprinting by Using Sliding-Window Reconstruction and Image Registration. Proceedings of the 25th Annual Meeting of ISMRM, Honolulu, Hawii, USA. 2017. p. 1273.
[16] Yu Z, Zhao T, Assländer J, Lattanzi R, Sodickson DK, A. CM. Exploring the sensitivity of magnetic resonance fingerprinting to different types of motion and possible correction mechanisms. Proceedings of the 25th Annual Meeting of ISMRM, Honolulu, Hawii, USA. 2017. p. 3938.
[17] Maes F, Collignon A, Vandermeulen D, Marchal G, Suetens P. Multimodality image registration by maximization of mutual information. IEEE Trans Med Imaging 1997;16(2):187–98.
[18] Fu ZW, Wang Y, Grimm RC, Rossman PJ, Felmlee JP, Riederer SJ, et al. Orbital navigator echoes for motion measurements in magnetic resonance imaging. Magn Reson Med 1995;34(5):746–753.
[19] Jiang Y, Ma D, Seiberlich N, Gulani V, Griswold MA. MR fingerprinting using fast imaging with steady state precession (FISP) with spiral readout. Magn Reson Med 2015;74(6):1621–31.
[20] Winkelmann S, Schaeffter T, Koehler T, Eggers H, Doessel O. An Optimal Radial Profile Order Based on the Golden Ratio for Time-Resolved MRI. Magn Reson Med 2007;26(1):68–76.
[21] Kim YC, Narayanan SS, Nayak KS. Flexible retrospective selection of temporal resolution in real-time speech MRI using a golden-ratio spiral view order. Magn Reson Med 2011;65(5):1365–1371.
[22] Stemmer A, Jellus V, Kannengiesser S, Kiefer B. Channel compression for BLADE. Proceedings of the 16th Annual Meeting of ISMRM, Toronto, Canada. 2016. p. 1274.
[23] Huang F, Vijayakumar S, Li Y, Hertel S, Duensing GR. A software channel compression technique for faster reconstruction with many channels. Magn Reson Imaging 2008;26(1):133–41.
[24] Fessler JA. On NUFFT-based gridding for non-Cartesian MRI. J Magn Reson 2007;188(2):191.
[25] Uecker M, Lai P, Murphy MJ, Virtue P, Elad M, Pauly JM, et al. ESPIRiT-an eigenvalue approach to autocalibrating parallel MRI: Where SENSE meets GRAPPA. Magn Reson Med 2014;71(3):990–1001.
[26] Chen Z, Xia L, Liu F, Wang Q, Li Y, Zhu X, et al. An improved non-Cartesian partially parallel imaging by exploiting artificial sparsity. Magn Reson Med 2016;78(1):271–9.
[27] Chen Z, Kang L, Xia L, Wang Q, Li Y, Hu X, et al. Technical Note: Sequential Combination of Parallel Imaging and Dynamic Artificial Sparsity Framework for Rapid Free-breathing Golden-Angle Radial Dynamic MRI: K-T ARTS-GROWL. Med Phys 2017;45(1):202–213.
[28] Twining CJ, Cootes T, Marsland S, Petrovic V, Schestowitz R, Taylor CJ. A Unified Information-Theoretic Approach to Groupwise Non-rigid Registration and Model Building. International Conference on Information Processing in Medical Imaging. 2005. p. 1–14.
[29] Ma D, Jiang Y, Chen Y, McGivney D, Mehta B, Gulani V, et al. Fast 3D magnetic resonance fingerprinting for a whole-brain coverage. Magn Reson Med 2017;79(1):2190–7.
[30] Liao C, Bilgic B, Manhard MK, Zhao B, Cao X, Zhong J, et al. 3D MR fingerprinting with accelerated stack-of-spirals and hybrid sliding-window and GRAPPA reconstruction. Neuroimage 2017;162(1):13–22.
[31] Ooi MB, Krueger S, Thomas WJ, Swaminathan SV, Brown TR. Prospective real-time correction for arbitrary head motion using active markers. Magn Reson Med 2009;62(4):943–54.
[32] Aksoy M, Forman C, Straka M, Skare S, Holdsworth S, Hornegger J, et al. Real-time optical motion correction for diffusion tensor imaging. Magn Reson Med 2011;66(2):366–378.
[33] Maclaren J, Herbst M, Speck O, Zaitsev M. Prospective motion correction in brain imaging: A review. Magn Reson Med 2013;69(3):621–36.